NOTES AND CORRESPONDENCE

Preliminary Experiments on the Scattering of Polarized Laser Light by Ice Crystals

KUO-NAN LIOU, R. BALDWIN AND T. KASER

Department of Meteorology, University of Utah, Salt Lake City 84112

8 September 1975

ABSTRACT

Preliminary experiments on the scattering of polarized He-Ne laser light by ice crystals and water droplets have been carried out in an environmental cold chamber. Experimental results reveal that the angular scattering diagrams of hexagonal plates and needles in the vertical polarization direction exhibit no specific features of maximum intensities such as rainbows, which are caused by internal reflections of the light rays within the spherical water droplets. The distinct scattering patterns between ice crystals and water droplets are much more pronounced than had been previously believed. The scattered radiance for plates and needles increases with increasing scattering angle from about 120° to 170°. Although the scattering of red light by plates generates a number of strong individual spikes for both vertical and horizontal polarization components, the backscattering patterns of plates and needles show no significant differences.

1. Introduction

Although the scattering of light by water clouds consisting of spherical water drops is well known (see, e.g., Deirmendjian, 1969), radiation problems related to ice crystals that are typical of those in cirrus clouds are far from resolved. Ice clouds are composed of nonsymmetrical ice crystals whose shapes and sizes vary with atmospheric conditions. The determination of polarized light scattered by ice particles is made very difficult owing to their nonsphericity and the consequent problem of orientation. Knowledge of the scattering-phase-matrix of a volume of ice crystals is of vital importance for the purpose of remote sensing of cloud compositions of the planet by means of radiance and polarization techniques as well as for radiation budget studies in cloudy atmospheres.

Theoretical studies of the scattering of an individual particle were reported by Wait (1955), Greenberg *et al.* (1967), Kerker (1969) and Liou (1972a) for cylinders, and by Asano and Yamamoto (1975) for spheriods. Jacobowitz (1971) obtained the phase function of an infinitely long hexagonal cylinder by means of geometrical ray tracing. Liou (1972b) further extended the scattering problem to a sample of cylinders with orientations and sizes taken into consideration. With respect to the experimental side, the reports by Huffman and Thursby (1969) and Huffman (1970) are apparently the only sources concerning the angular scattering measurements for ice crystals. In their experiments, a zirconium light source with a wavelength of 0.5 μm was employed. The effect of polarization was not included and the experiments were carried out to the scattering angle of 150°. Field experiments for the measurement of the polarization of sunlight by ice-crystal clouds were also reported recently by Hansen and Coffeen (1974).

On the basis of the theoretical (Liou, 1972b) and experimental (Huffman and Thursby, 1969) investigations, it seems to have been established qualitatively that the scattering behavior of nonspherical ice crystals is different from that of water droplets. Ice crystals scatter more light in the vicinity of the 90° scattering angle at the expense of the scattering at forward and backward directions. It is the purpose of this note to report some experiments that we have carried out at the University of Utah concerning the scattering of polarized light by laboratory generated water-droplet and ice-crystal clouds. Results of the angular scattering diagram for water droplets and ice crystals reveal that a drastic difference is found in scattering angles from about 90° to 160°.

2. Theoretical consideration

If a fixed coordinate system is arranged in such a way that the polarizers in both the transmitter and receiver are in the same directions with respect to a fixed plane, then the Stokes parameters of the scattered

light in units of radiance may be written as (Liou, 1975)

$$\mathbf{I}(\theta)=C\mathbf{M}(\theta)\mathbf{F}_0, \tag{1}$$

where C is a constant of proportionality. The incident wave in units of flux density is given by

$$\mathbf{F}_0=\begin{bmatrix} F_{0l} \\ F_{0r} \\ U_0 \\ V_0 \end{bmatrix}, \tag{2}$$

where l and r denote polarization components in the horizontal and vertical directions, respectively, and the phase matrix (van de Hulst, 1957) may be expressed as

$$\mathbf{M}(\theta)=\begin{bmatrix} M_2 & M_3 & S_{23} & -D_{23} \\ M_4 & M_1 & S_{41} & -D_{41} \\ 2S_{24} & 2S_{31} & (S_{21}+S_{34}) & (-D_{21}+D_{34}) \\ 2D_{24} & 2D_{31} & (D_{21}+D_{34}) & (S_{21}-S_{34}) \end{bmatrix}. \tag{3}$$

The symbols M, S and D are values associated with the complex combination of the four amplitudes [see van de Hulst (1957, p. 44) for the comprehensive definitions]. We note that these elements represent the optical properties of the scattering medium with respect to the incident wavelength and the scattering angle θ.

For spherical water droplets, the non-zero elements are M_1, M_2, S_{21} and D_{21}. Thus if a horizontally polarized light is used as the incident radiation source, then

$$\mathbf{I}=CF_{0l}\begin{bmatrix} M_2 \\ 0 \\ 0 \\ 0 \end{bmatrix}. \tag{4}$$

For incident vertically polarized radiation, on the other hand, the scattered radiance is given by

$$\mathbf{I}'=CF_{0r}\begin{bmatrix} 0 \\ M_1 \\ 0 \\ 0 \end{bmatrix}. \tag{5}$$

Note that the M_1 and M_2 components can be evaluated exactly from the well-known Mie scattering theory (Mie, 1908).

However, for nonspherical ice crystals, if no assumptions are made on their physical positions, then the scattered radiances corresponding to the above two cases are respectively,

$$\mathbf{I}=CF_{0l}\begin{bmatrix} M_2 \\ M_4 \\ 2S_{24} \\ 2D_{24} \end{bmatrix}. \tag{6}$$

$$\mathbf{I}'=CF_{0r}\begin{bmatrix} M_3 \\ M_1 \\ 2S_{31} \\ 2D_{31} \end{bmatrix}. \tag{7}$$

The scattering behaviors of the M_1 and M_2 components for water droplets and ice crystals generated in the laboratory will be investigated in the following experiments.

3. Experimental arrangement

The experiments were performed in an environmental cold chamber which could be cooled down to about −20°C. The chamber is 3.33 m by 2.72 m wide with a height of 2.34 m. The angular apparatus described below and shown in Fig. 1 is placed within the center of the cold chamber. The nephelometer system consists of an alumina arm, which can be moved around the horizontal plane by a motor beneath. The speed of the rotating arm is controlled by a motor power supply outside the cold room. On the driving arm, there is a photomultiplier tube (PMT) and a housing unit with a collimator in front of it. A polarizer, which can be rotated exactly 90°, is also located in front of the collimator, so that the scattered radiation can be detected in the horizontal and vertical polarization directions. The radiation source employed in this study is a He-Ne unpolarized Spectra Physics laser whose output power is 0.1 mW. A rotating polarizer was placed in front of the laser to produce the desirable incident polarization. Along the line of the laser beam there is a light trap. A large portion of the wall of the cold chamber is covered by the black cloth so as to avoid possible reflection interference. Furthermore, a fixed reference PMT and housing located at about 15° scattering angle is also employed to denote the possible concentration variations of cloud particles.

The electronic components for the detection are connected through a circulation duct near the left-side bottom of the cold chamber. They are placed in an instrument rack. The components include a power supply and a picoameter for the rotating PMT and housing. The rotating PMT signal is recorded on an X-Y chart recorder. The picoameter is used for the purpose of amplification and time averaging. The reference PMT is also connected to a power supply and a picoameter. The reference signal and the angular indication are recorded on a two-channel strip-chart recorder.

The timing for one scan (0° to 180°) takes from about 18 s to about 9 min. In view of the rapid changes of ice-crystal clouds and the required time average, it was decided to use a time duration of about 4 min per scan. The electronic monitoring and control components are located outside the cold room; when its window is covered by a black cloth, the experiment can be conducted with the exterior light on.

With respect to the cloud physics, the water-droplet cloud is continuously produced by boiling water, utilizing a heater in an open container. The heater is connected to a Variac, so that the rate of water vapor flow to the cold room can be reduced when it is desirable. The temperature of the cold room is normally about −5°C to about −15°C during experiments. Liquid

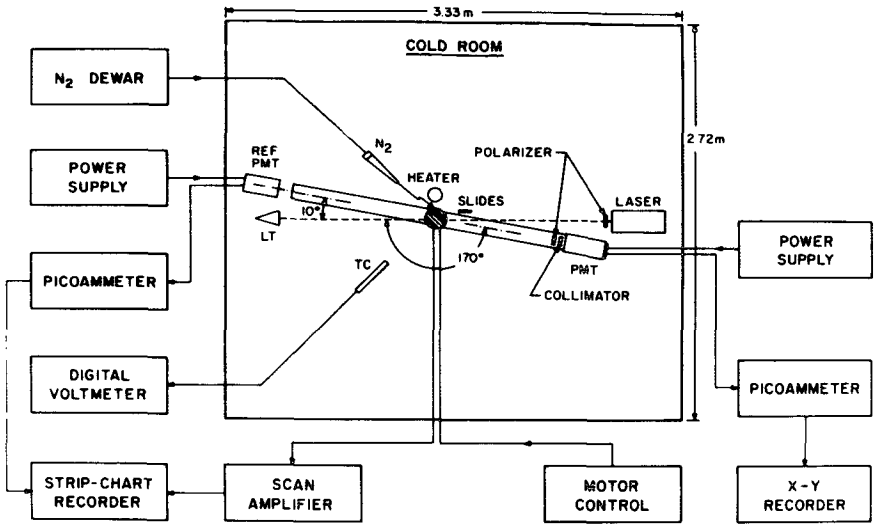

FIG. 1. Plan view of the cold room arrangements and block diagrams of the electronic components.

nitrogen, introduced into the cold room from an exterior dewar through a tube located above the scattering apparatus, was used for ice crystal nucleation. Before the experiment begins, a number of glass slides coated with 1% solution of polyvinyl formula dissolved in ethylene dichloride (Schaefer, 1962) were prepared and placed on the scattering table.

4. Experimental results

Our primary purpose here is to report the different scattering behavior between spherical water droplets and nonspherical ice crystals, and between hexagonal plates, and needles and columns. Thus, we select three representative scattering diagrams of water droplets and ice crystals for illustration purposes.

a. Experiment 1

A water cloud was first produced in the cold room. After the signal recorded by the reference PMT reached an almost steady level, liquid nitrogen was introduced. It was turned off after about 20 s, and the angular scattering measurement was then carried out. The *in-situ* temperature above the optical table was about −10 to −15°C during the first stage of the experiment. Fig. 2 depicts the scattering diagram from about 30° to 170° scattering angles, along with the reference signal recorded at the scattering angle of 15°. The time scale of the scan is shown at the bottom of the diagram. The laser beam and the detector are vertically polarized. Thus the scattered radiance measured corresponds to the M_1 component illustrated previously. The replicas taken during this experiment show that ice crystals captured are predominately plates whose sizes along the major axis vary from about 10 to 50 μm (Fig. 3a). The scattering diagram shown in the left-hand side of Fig. 2 exhibits a number of spiking events which are thought to be produced by external reflections of the large basal faces of the plate crystals. The scattered radiation in a relative linear scale decreases to a scattering angle of about 120°, and increases to the backward directions with no specific maximum in-

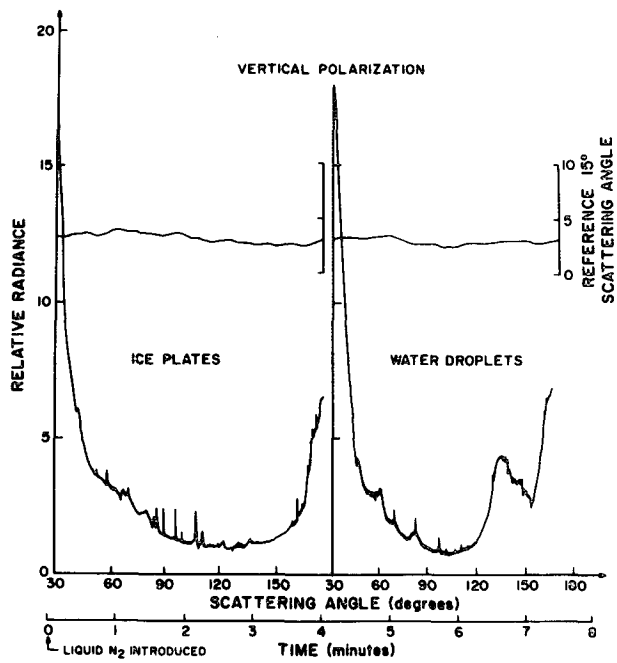

FIG. 2. Angular scattering diagrams (in relative radiance units) of hexagonal plates and water droplets illuminated by 0.6328 μm He-Ne laser light. The laser beam and detector are vertically polarized. The reference signals recorded at a scattering angle of 15° are displayed in the upper part of the figure. The bottom scale corresponds to the time of two scans.

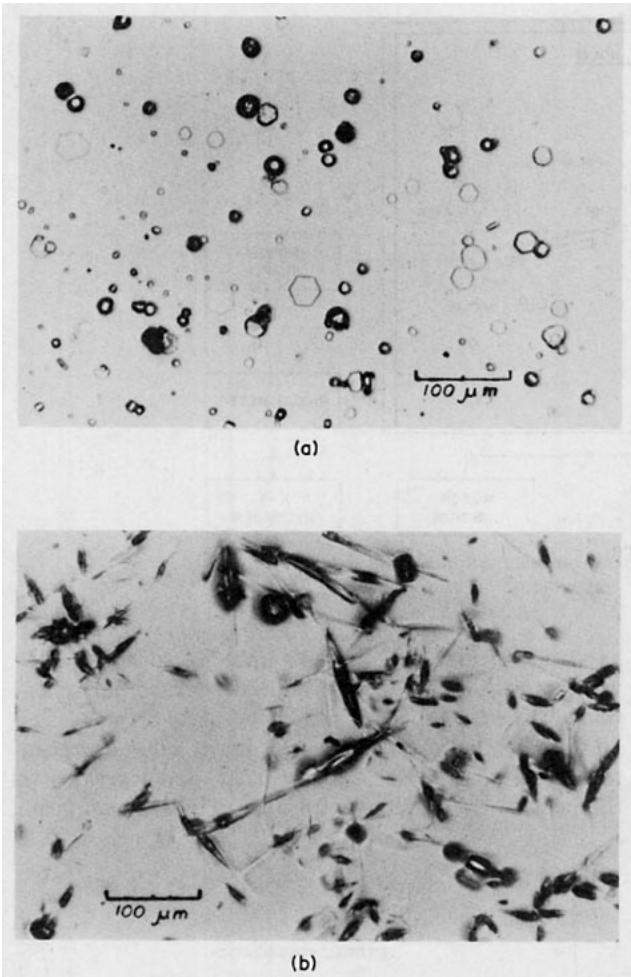

FIG. 3. Replicas of hexagonal plates and prisms (a) corresponding to the scattering results presented in Figs. 2 and 4, and of needle type crystals (b) corresponding to the scattering results presented in Fig. 5.

tensity features observed. Another scan was immediately taken, while the water vapor was continuously supplied to the cold room. Its temperature rose to about 0°C, and the cloud at this point was primarily composed of water droplets. Individual spiking events shown in scattering angles less than about 100° indicate that the cloud also consists of a number of plates which eventually fall out due to sedimentation. A well-defined rainbow feature, which is caused by the light rays undergoing one internal reflection within the spherical water droplets, is shown at a scattering angle of about 135°. We note that the reference signals during these two scans remain at about the same level. This implies that the concentration of cloud particles has been maintained at a constant value. On the basis of these two scattering diagrams and the steady reference signals, it is evident that ice plates scatter more light near a scattering angle of about 100°, and that ice plates produce no maximum intensity at the rainbow angle. A number of other scattering scans for ice plates support these findings.

b. Experiment 2

The polarizers in front of the laser and the detector were changed to the horizontal direction, so that the scattered radiance measured corresponds to the M_2 component as described in Section 2. The same procedures for producing water and ice clouds and for the angular scattering scan used in Experiment 1, were carried out. The *in-situ* temperature above the optical table was maintained at about −10 to −15°C. The graph on the left-hand side of Fig. 4 represents the scattering diagram of hexagonal plates, which resemble those illustrated in Fig. 3a. A number of similar individual spikes are shown in regions from 60° to 100° scattering angles. The scattered radiances from about 50° to 90° apparently are smaller than those of the vertical polarization component. Although these differences are also noticed in other scans, the physical reason for it is not clear to us at this time. The right-hand side of this figure depicts the scattering diagram of the cloud composed primarily of water droplets. Evidently a dense water cloud was produced as can be seen from the increased reference signals. As a result, the scattered radiances of water droplets near 90° to 150° scattering angles are greater than those of ice plates. The scattering patterns of both ice and water particles for the horizontal polarization component reveal no features of maximum intensities. We hope that simultaneous scattering measurements for both vertical and horizon-

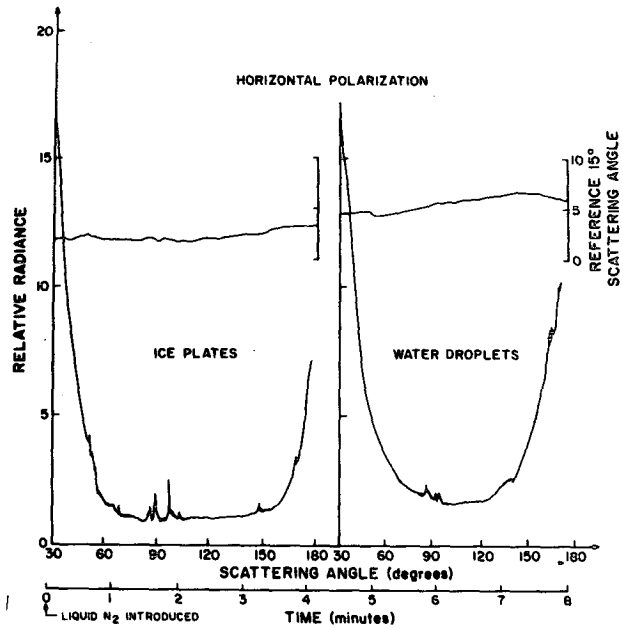

FIG. 4. As in Fig. 2, except that the laser beam and detector are horizontally polarized. (Note that the second scan was delayed by about 20 s.)

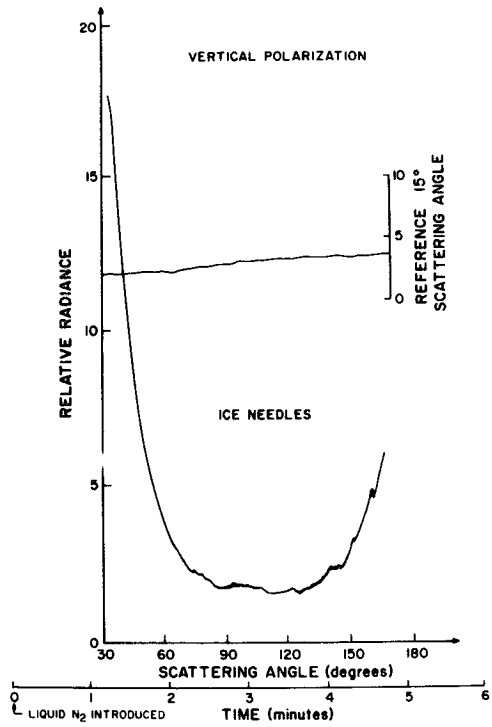

FIG. 5. The angular scattering diagram of needles illuminated by the He-Ne laser light. The laser beam and detector are vertically polarized.

tal polarization components may be obtained in future experiments.

c. Experiment 3

This experiment investigated the possible differences of the light scattering behavior between plate and needle types of ice crystals. In order to generate needles, the *in-situ* temperature above the optical table was reduced to about −3 to −8°C. The ice crystals captured during this experiment are displayed in Fig. 3b. The sizes of ice needles along the major axis are from about 50 to 100 μm. Fig. 5 shows the results of the scattering scan for the vertical polarization component. Scattering by needles produced no spiking events during this experiment. Aside from this difference, no specific features may be utilized to differentiate between plates and needles.

5. Conclusions

The preliminary experimental results indicate that the angular scattering of the vertically polarized laser beam by hexagonal plates and needles produces no specific features of maximum intensities in the region of 30° to 170° scattering angles. The distinct differences in scattering behavior between ice crystals and water droplets are much more pronounced than had previously been reported. The scattering of red light by hexagonal plates exhibits a number of individual spiking events, which generate sufficient strength to be registered by the chart recorder above signal noise levels. In addition, the scattered radiance for nonspherical ice plates and needles apparently increases with increasing scattering angle from about 120° to 170°. For both vertical and horizontal polarization components, the backscattering patterns of plate and needle types of crystals show no significant differences.

Acknowledgments. We are very grateful to Prof. C. H. Wang and Mr. S. Hunter of the Chemistry Department, University of Utah, for assistance in various aspects of the experiment, particularly for the loan of the picoameter and *X-Y* chart recorder. This research was supported by the Atmospheric Sciences Section of the National Science Foundation under Grant DES-75-05216. The Research Committee of the University of Utah also provided funds for a number of optical and electronic equipment items used in this investigation.

REFERENCES

Asano, S., and G. Yamamoto, 1975: Light scattering by a spheroidal particle. *Appl. Opt.*, **14**, 29–49.

Deimendjian, D., 1969: *Electromagnetic Scattering on Spherical Polydispersion.* Elsevier, 290 pp.

Greenberg, J. M., A. C. Lind, R. T. Wang and L. F. Libelo, 1967: Scattering by nonspherical system. *Electromagnetic Scattering*, R. L. Rowell and R. W. Stein, Eds., Gordon and Breach, 842 pp.

Hansen, J. E., and D. L. Coffeen, 1974: Analysis of cloud polarization measurements. *Preprints Conf. Cloud Physics*, Tucson, Ariz., Amer. Meteor. Soc., 350–356.

Huffman, P., 1970: Polarization of light scattered by ice crystals. *J. Atmos. Sci.*, **27**, 1207–1208.

——, and W. R. Thursby, Jr., 1969: Light scattering by ice crystals. *J. Atmos. Sci.*, **26**, 1073–1077.

Jacobowitz, H., 1971: A method for computing the transfer of solar radiation through clouds of hexagonal ice crystals. *J. Quant. Spectros. Radiative Transfer*, **11**, 691–695.

Kerker, M., 1969: *The Scattering of Light and Other Electromagnetic Radiation.* Academic Press, 666 pp.

Liou, K. N., 1972a: Electromagnetic scattering by arbitrarily oriented ice cylinders. *Appl. Opt.*, **11**, 667–674.

——, 1972b: Light scattering by ice clouds in the visible and infrared: A theoretical study. *J. Atmos. Sci.*, **29**, 524–536.

——, 1975: Theory of the scattering-phase-matrix determination for ice crystals. *J. Opt. Soc. Amer.*, **65**, 159–162.

Mie, G., 1908: Beigrade für Optik trufen Medien speziell kolloidaler Metallosungen. *Ann. Phys.*, **25**, 377–445.

Schaefer, V. J., 1962: The vapor method for making replicas of liquid and solid aerosols. *J. Appl. Meteor.*, **1**, 413–418.

van de Hulst, H. C., 1957: *Light Scattering by Small Particles.* Wiley, 470 pp.

Wait, J. R., 1955: Scattering of a plane wave from a circular dielectric cylinder at oblique incidence. *Can. J. Phys.*, **33**, 189–195.